INT. J. ELECTRONICS, 2004, VOL. ??, NO. ??, 1–21

Taylor & Francis
Taylor & Francis Group

Control of power electronic interfaces in distributed generation Microgrids

A. ARULAMPALAM†, M. BARNES‡*, A. ENGLER§,
A. GOODWIN¶ and N. JENKINS‡

Technological advances and environmental pressures are driving the interconnection of renewable energy sources to the distribution network. The interconnection of large amounts of non-traditional generation however causes problems in a network designed for 'conventional' operation. The use of power electronics interfaces and the 'bundling' of micro-generation and loads into so-called Microgrids, offers a potential solution. Each Microgrid is designed to operate as a 'good citizen' or near ideal conventional load. This paper discusses the various elements of the new Microgrid concept and presents suggestions for some typical control strategies for the various system elements.

Nomenclature

All main variables are defined in Figure 3 except those listed below.

Fsystemmax	Maximum limit of frequency under P–f droop control
Fsystemmin	Minimum limit of frequency under P–f droop control
Fsystemref	Reference frequency for inverter with no injected Watts
Pgen	Generator real output power
Pload	Load real power
Pvsc_output	Real power output from energy-storage unit inverter
Qgen	Generator reactive output power
Qload	Load reactive power
Qvsc_output	Reactive power output from energy-storage unit inverter
Vtmag	Magnitude of terminal voltage under Q–V droop control
Vtmax	Maximum limit of terminal voltage under Q–V droop control
Vtmin	Minimum limit of terminal voltage under Q–V droop control
Vtrms	RMS terminal voltage
Vtref	Reference terminal voltage for inverter with no injected VArs

Received 8 November 2003. Accepted 29 June 2004.

* Author for correspondence. e-mail: mike.barnes@umist.ac.uk
†Department of Electrical and Electronic Engineering, University of Peradeniya, Sri Lanka.
‡Department of Electrical and Electronic Engineering, UMIST, UK.
§Institut für Solare Energieversorgungstechnik, Kassel, Germany.
¶Urenco Power Technologies Ltd., Capenhurst, UK.

International Journal of Electronics ISSN 0020–7217 print/ISSN 1362–3060 online © 2004 Taylor & Francis Ltd
http://www.tandf.co.uk/journals
DOI: 10.1080/00207210412331289023

1. Introduction

Modern power network operators are having to respond to a number of challenges: load growth and changes in the geographical distribution of customers on the one hand; new environmental policy and the usual economic pressures of the marketplace on the other. Uprating infrastructure to solve the former two problems is constrained by the latter two. Indeed the extension of the transmission network is now usually not possible due to an (understandable) 'not in my back-yard' (NIMBY) attitude by the local community. All this and a multi-national commitment to reduce CO_2 emissions, has led to increased interest in the local connection of renewable energy generation and combined heat and power (CHP) at the distribution level.

In principle this distributed generation (DG) can ease pressure on the transmission system capacity by supplying some of the local load. In reality there are technical limits on the degree to which distributed generation can be connected, especially for some intermittent forms of renewable generation and weaker areas of the distribution network. This limit principally stems from the original design philosophy of the power system. The distribution network was intended to cope with conventional loads being supplied from central generation: a hierarchical flow of power from the transmission network down. Changing the power flow causes problems since DG does not behave in the same way as a conventional load.

The microgrid concept has been discussed as a potential means to combat problems caused by the unconventional behaviour of DG, increasing DG penetration (Lasseter *et al*. 2002 a). In essence a microgrid (figure 1) consists of a combination of generation sources, loads and energy storage, interfaced through fast acting power electronics. This combination of units is connected to the distribution network through a single point of common coupling (PCC) and appears to the power network as a single unit. The aim of operating Microgrid sub-systems is to move away from considering DG as badly behaved system components, of which a limited

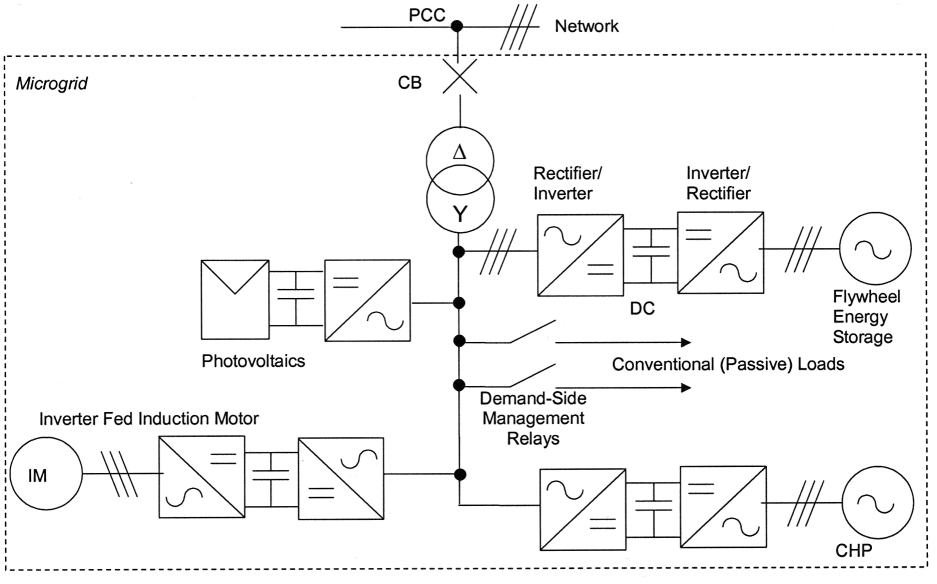

Figure 1. Simple example Microgrid.

amount can be tolerated in an area, to 'good citizens' (Lasseter 2001), i.e. an aggregate of generation and load which behave as nearly ideal conventional loads. Although the concept of using Microgrids to provide ancillary services to the local network has also been discussed, present commercial incentives are probably insufficient to encourage this.

A critical feature of the Microgrid is the power electronics. 'The majority of the microsources must be power electronic based to provide the required flexibility to ensure controlled operation as a single aggregated system' (Lasseter *et al.* 2002 a). Such as system must be capable of operating despite changes in the output of individual generators and loads. It should have 'plug-and-play' functionality: it should be possible to connect extra loads without reprogramming a central controller (up to a predefined limit). It should be possible that some of these are loads conventional. Likewise it must be possible to add generation capacity with minimal additional complexity. Key, immediate issues for the microgrid are power flow balancing, voltage control and behaviour during disconnection from the point of common coupling (islanding). Protection and stability also need to be considered, but are outside the scope of this article.

The most immediate sites for application of the Microgrid concept would be existing remote systems which consist of a bundle of microsources and loads (e.g. figure 2). It could be prohibitively expensive to compensate for load growth or poor power quality, by uprating the long supply line and the feeder to the (weak) source bus. Upgrading the local sub-system to a Microgrid could be a cheaper option. A necessary feature of such a Microgrid is that it can act as a semi-autonomous system, i.e. when the main network is not available, the Microgrid can still operate independently. This also has the potential to significantly improve the power quality of Microgrid systems by allowing them to ride through some faults. This is an advantage for sub-systems in larger installations requiring heterogeneous power quality.

To date Microgrids have been discussed as a concept (Lasseter *et al.* 2001, 2002 a,b). This paper discusses how some of the key power electronics control concepts might be realized. Specific issues discussed are:

- The implementation of power flow control (P and Q).
- Response to the onset of autonomous operation (islanding) and resynchronization.
- The requirement for energy storage.

An assumption used in this paper is that a central controller, or 'system optimizer' (Lasseter 2002 b) will be required to coordinate the power electronic

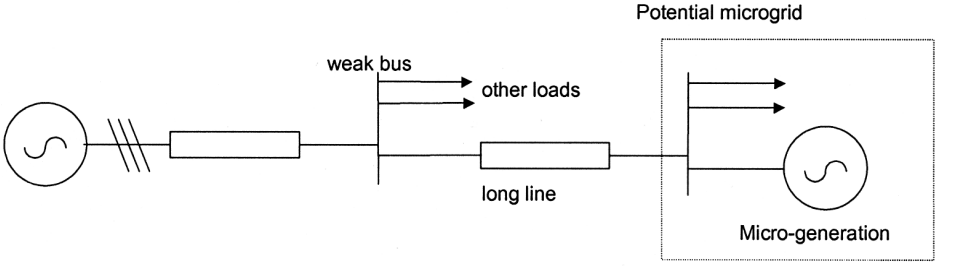

Figure 2. Potential Microgrid: remote combination of microsource(s) and loads.

interfaces in the Microgrids. This will be a slow acting outer control loop, the principle function of which is to determine the balance of steady-state real and reactive power flow between the Microgrid components and the network. The central controller communicates to the individual units by a comparatively low bandwidth (and hence inexpensive) link.

2. Overview of control of power electronics interfaces

Figure 3 shows the circuit diagram of the voltage source converter (VSC) system considered in this paper. For simplicity, a constant-voltage split dc link is shown, though this can be a link to any type of load, source or energy storage unit. The load was modelled as a main $(5+j3)\,\Omega$ load per phase with a switchable $(15+j9.4)\,\Omega$ load per phase in parallel. Initially these loads were balanced but, imbalance could be added by varying one phase impedance. The line impedance of the Microgrid was modelled by a very small resistance and reactance, since it was assumed that the elements of the Microgrid were in geographically close proximity. The PSCAD/EMTDC block-set for a synchronous generator was used with rated current of 60 A and a 1.2 MW/MVA inertia constant. Control of the voltage source inverter, which represents the energy storage unit, is described subsequently.

In this control concept three-phase instantaneous terminal voltages, load currents, VSC injected currents, required injected active and reactive powers, and three-phase instantaneous voltages on both side of the circuit breaker are measured and fed to the VSC control circuit. This circuit produces gate pulses to the VSC IGBT switches. This forces the VSC to inject the active and reactive power requested by the local controller. By suitable selection of injection voltage the unit can undertake voltage regulation, frequency regulation, unbalanced current compensation, respond

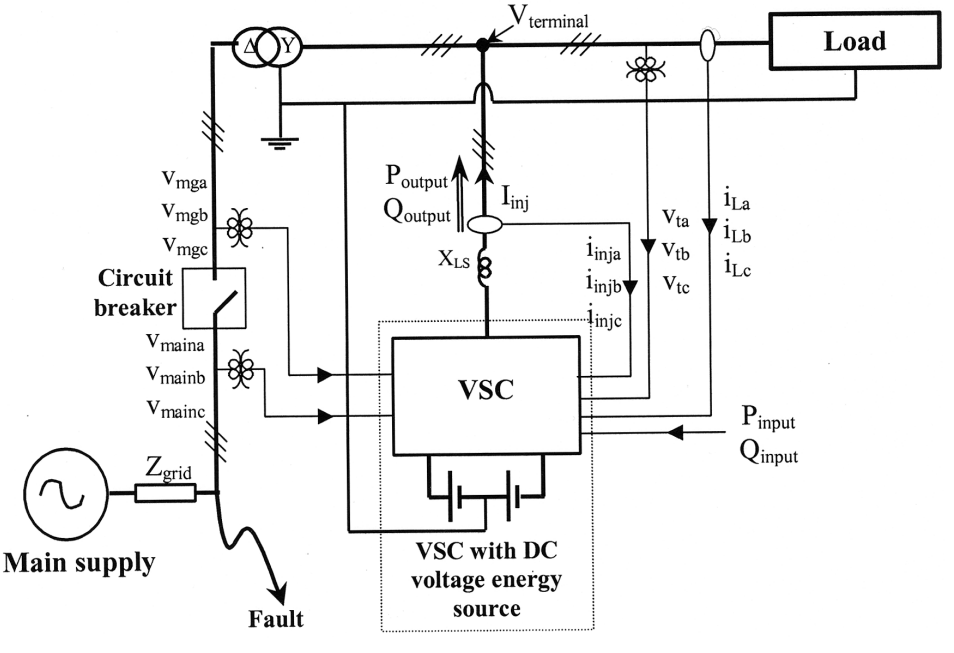

Figure 3. Circuit diagram of the overview of the VSC control and system simulated.

to commands sent by the central controller, and reconnect the micro grid to the main supply.

For simple inductive power systems, power flow is typically calculated in terms of sending end (V_s) and receiving end (V_r) voltages (figure 4) such that

$$P = \frac{V_s V_r}{X} \sin(\delta s - \delta r) \tag{1}$$

$$Q = \frac{V_s^2}{X} - \frac{V_s V_r}{X} \cos(\delta s - \delta r) \tag{2}$$

where P and Q are power into the line from the sending end.

If this voltage control concept is adopted for the control of inverters, it is difficult to avoid small imbalances in output voltage resulting in a net dc voltage injection. This can lead to a large dc current injection.

With current regulated control (figure 5), where the desired line current itself is calculated and controlled, this problem is eliminated. The sum of the currents calculated to control active and reactive power ($I_{\alpha\_pq}, I_{\beta\_pq}, I_{0\_pq}$) are then compared with the measured VSC currents ($I_{\alpha\beta 0\_\text{measured}}$), to obtain an error value. The output voltage of the VSC is adjusted to correct for this current error, and is calculated from

$$V_{\alpha\beta 0\_\text{error}} = L \cdot \frac{\mathrm{d}i}{\mathrm{d}t} = L \frac{I_{\alpha\beta 0\_\text{pq}} - I_{\alpha\beta 0\_\text{measured}}}{T_s} \tag{3}$$

where L is the coupling inductance and T_s is the switching period. The VSC $\alpha\beta 0$ output voltage components are fed as inputs to a three-dimensional space-vector pulse-width modulation (SVPWM) generator to produce gate pulses to the VSC switching devices. This allows the VSC to inject the current required by the system control.

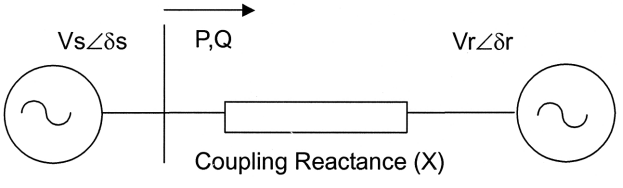

Figure 4. Short-line power system model.

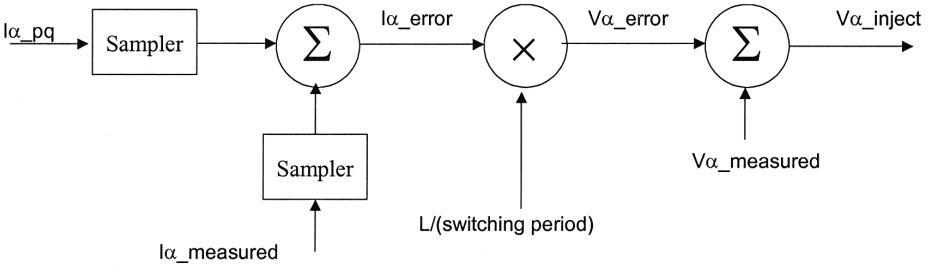

Figure 5. Current regulated control, shown for α component (β and 0 components function in the same way).

3. Microgrid reactive power control

As a good approximation, many conventional power systems are mainly inductive, i.e. have a high ratio of reactance to resistance (X/R ratio). For such systems, equation (2) tells us that differences in voltage cause reactive power flows, or conversely, reactive power flows influence terminal voltage. Typically therefore reactive power is controlled by a Q vs. V droop line (figure 6) (Tyll and Bergmann 1990, Chandorkar *et al.* 1993).

Figure 7 shows the block diagram of the voltage regulation control technique. Three-phase terminal voltages (V_{ta}, V_{tb}, V_{tc}) are measured and fed as inputs to the controller. The magnitude of the terminal voltage vector (Vtmag) is calculated and compared with the set reference value (Vtref = 415 V). The error voltage is filtered using a low pass filter and multiplied by a gain constant to obtain droop control of the VSC. The output of the voltage regulation control block gives the reactive power (QinjV) that needs to be injected to maintain the terminal voltage according to droop set value.

Figure 8 shows simulation results with and without the voltage regulation control technique, for an abrupt reduction in the PCC voltage at the end of the long supply feeder to which the Microgrid is connected. The Microgrid, in this case the VSC of the energy storage unit, injects reactive power to maintain the rms terminal voltage (Vtrms) within the acceptable limits.

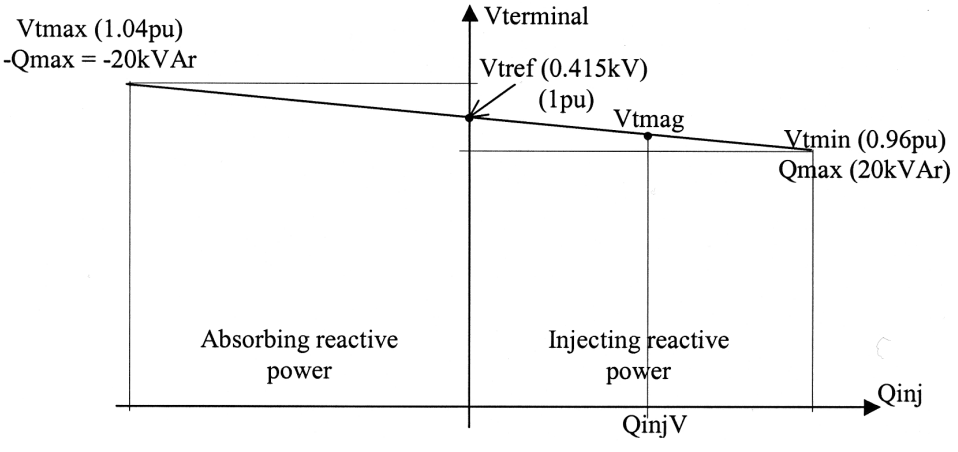

Figure 6. Droop control of the VSC terminal voltage.

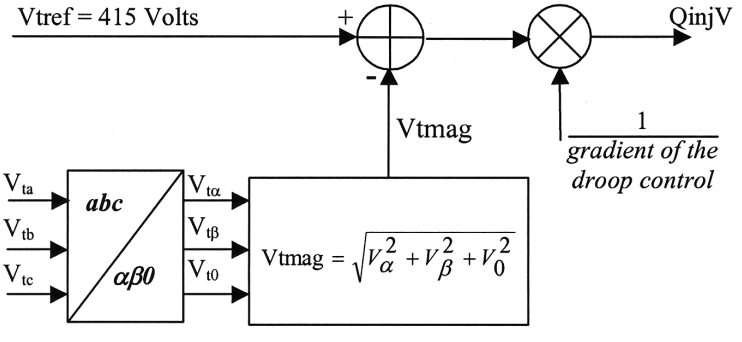

Figure 7. Block diagram of the VSC control for voltage regulation.

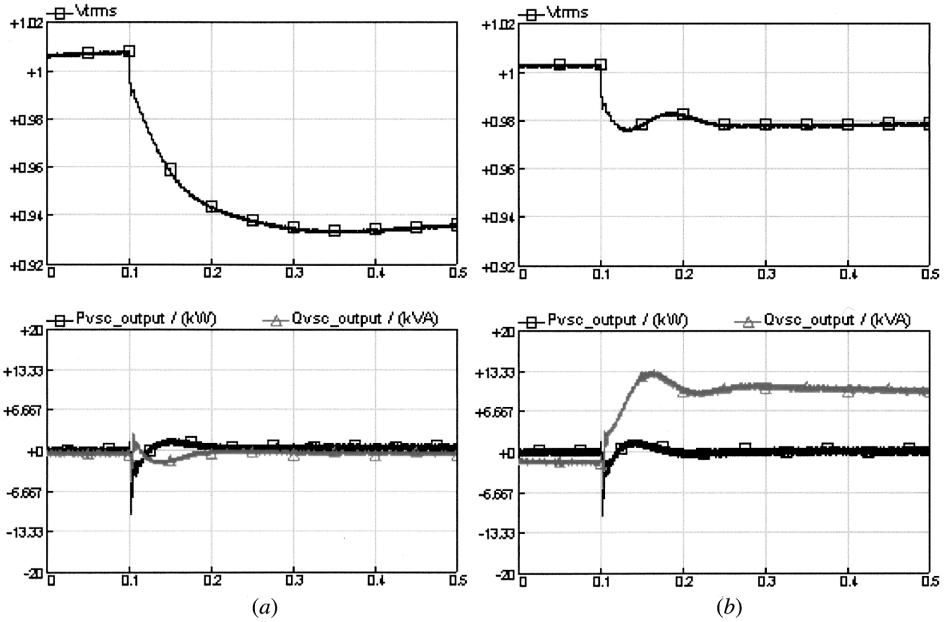

Figure 8. Simulation results (*a*) without and (*b*) with the voltage regulation control (Microgrid connected to main supply).

The central controller effectively sets the droop line slope of the individual VSC interfaces, to determine reactive power sharing between the units and the reactive power export/import of the Microgrid under steady-state operation. During islanded operation the net reactive power flow will be zero. Ideally, the voltage in the Microgrid will increase (if there is excess reactive power), forcing power electronic units to produce less Q or even absorb reactive power, until a new steady-state voltage is reached (net zero Q flow).

4. Microgrid real power flow

For conventional systems there is an interrelation between real power and the derivative of phase, i.e. frequency. Should there be an excess of real power in the system, the kinetic energy of the generator rotors increases, increasing the system frequency. The generator controllers would then reduce the real power supply to bring the frequency back into line. The converse occurs when there is a shortage of real power. In a similar manner a power versus frequency droop line can be used to determine real power output by a VSC (figure 9). If the system frequency is too high the output power can be reduced. If the system frequency is too low more power can be exported, up to the limits of the VSC.

4.1. *Real power vs. frequency control*

The direct control system analogy of the droop line is to measure system frequency and control real power (figure 10). System frequency is measured from a phase locked-loop (PLL), which operates based on three-phase terminal voltage. The system frequency is compared with a reference value (typically 50 Hz under

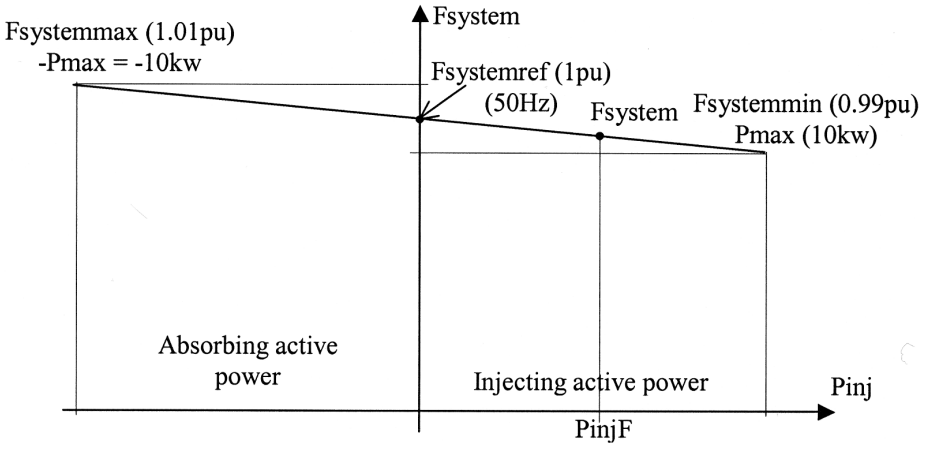

Figure 9. Droop control of the Microgrid system frequency.

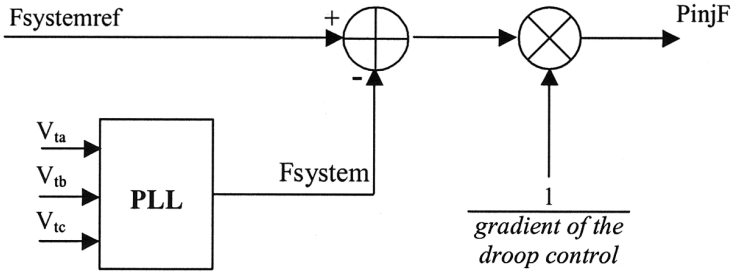

Figure 10. Block diagram of the VSC control for frequency regulation.

normal operation). The frequency deviation is filtered using a low pass filter and multiplied by a gain constant to obtain droop control (Chandorkar *et al.* 1993, Johnson *et al.* 1994, Lasseter 2002 b).

Figure 11 shows simulation results with the voltage and frequency regulation control technique, in response to an abrupt change in load when Microgrid was operated in island mode. The VSC injects active and reactive power to maintain the terminal voltage and the Microgrid system frequency within the acceptable limits.

4.2. *Frequency vs. real power control*

In a real system obtaining an accurate measurement of instantaneous frequency is not straightforward. Measuring instantaneous real power is easier. It has therefore been proposed (Engler *et al.* 2001, Engler 2003) that the control discussed in § 4.1 be reversed: the VSC output power is measured and this quantity is used to adjust its output frequency.

For the experiment, three SMA Sunny Island^{TM} inverters programmed with this scheme (rated power 3.3 kW, switching frequency 16 kHz, coupling inductor 0.8 mH) were connected on a single phase to an ohmic load, each via a thin (approx. 10 m) low voltage cable. The frequency droop of the inverters denoted by L1, L2 in figure 12 was set to 1 Hz/rated power. The inverter denoted with L3 was set to 2 Hz/rated power. It is evident that this method allows L3 to supply a smaller

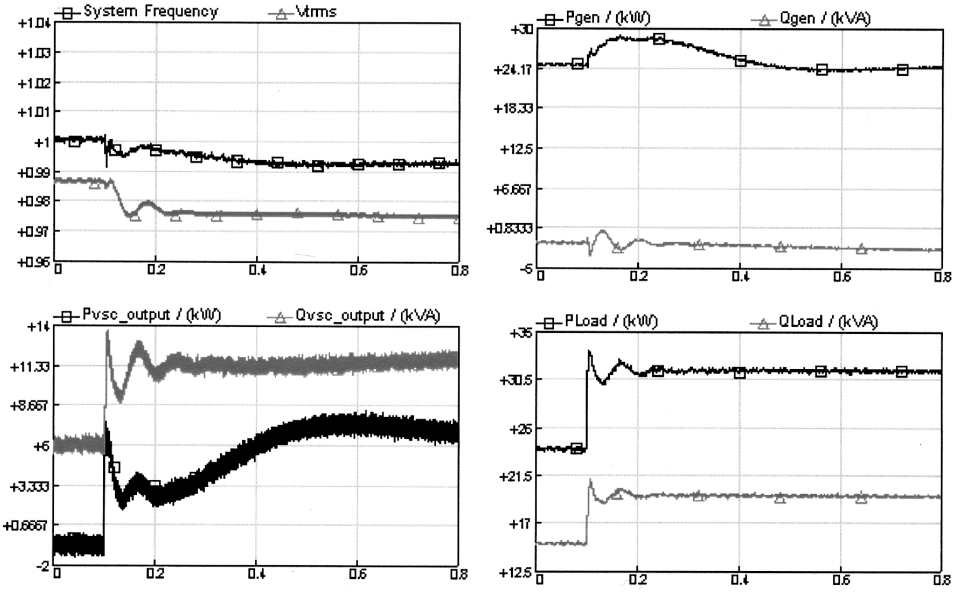

Figure 11. Simulation results with the voltage and frequency regulation control (during island operation of the Microgrid).

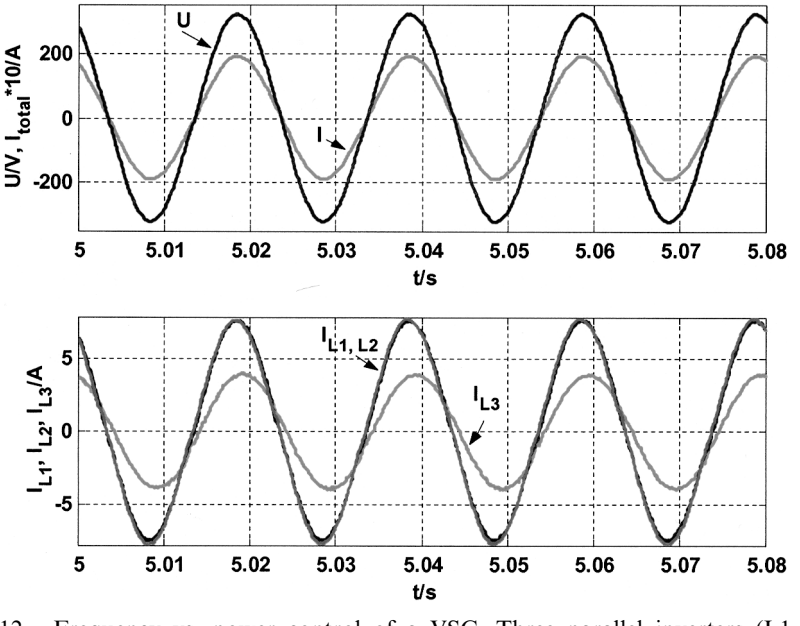

Figure 12. Frequency vs. power control of a VSC. Three parallel inverters (L1, L2, L3) responding to steady 3 kW load, top: network voltage, U (V) and total current ($\times 10$ A), bottom:individual currents (A).

proportion of power in this case, and that the system is stable and responds quickly to changes in load (figure 13).

5. 'Good citizen' behaviour – power injection set by central controller

For the Microgrid to behave as a 'good citizen' and absorb/inject a specified amount of aggregate power the position of the droop lines of the individual VSCs must be adjusted by a central controller. This need not be a particularly fast control loop, since even a slow telecommunications link has time-constants significantly faster than most power network sub-systems. Additional active and reactive powers (Pinj, Qinj) to be injected in this case are set by the central controller for each specific VSC (figure 14). The active (PinjF) and reactive (QinjV) power set by

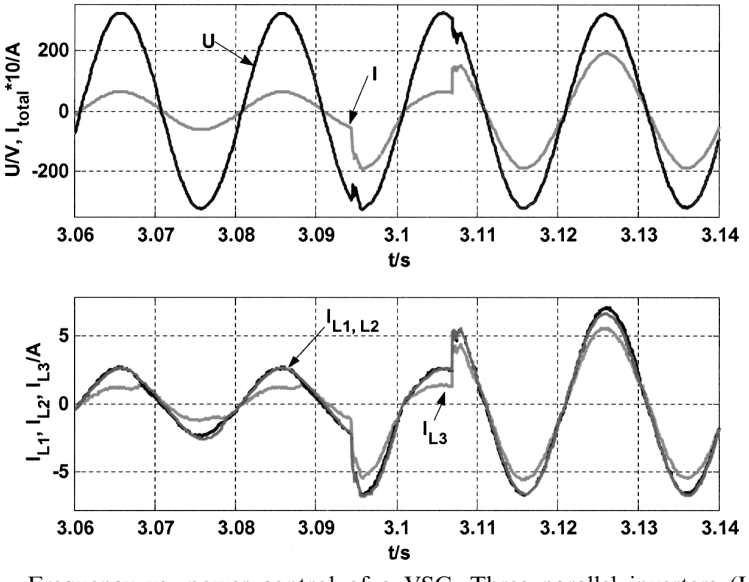

Figure 13. Frequency vs. power control of a VSC. Three parallel inverters (L1, L2, L3) responding to a change in load from 1 kW to 3 kW, top: network voltage, U (V) and total current ($\times 10$ A), bottom: individual currents (A).

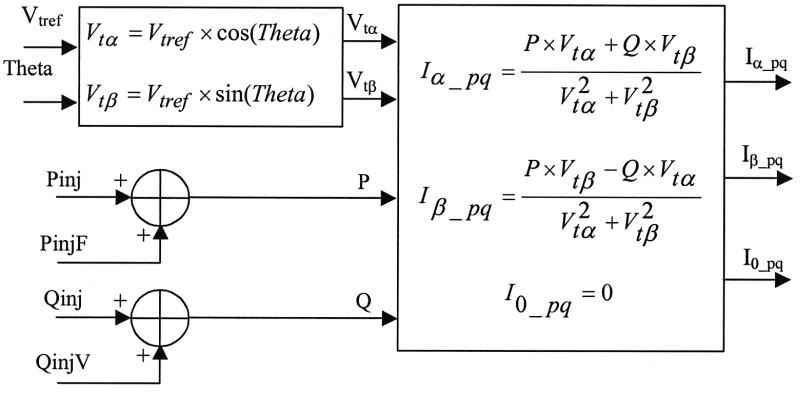

Figure 14. Block diagram of the VSC control for frequency regulation.

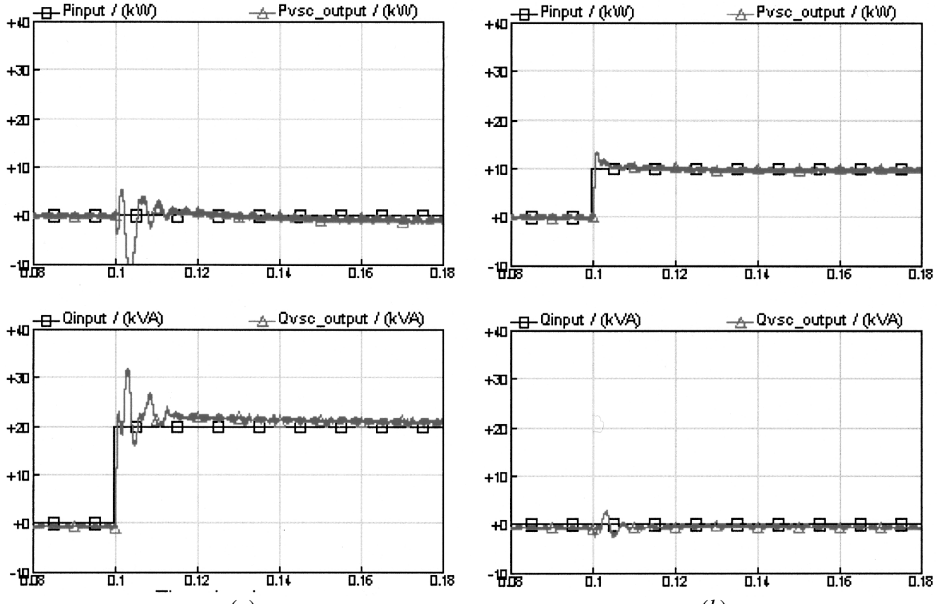

Figure 15. Simulation results with the active and reactive power control set by central controller (all other controls are disengaged and Microgrid is connected to the main supply), (*a*) Pinput = 0, Qinput = 20 kVAr, (*b*) Pinput = 10 kW, Qinput = 0 kVAr.

the frequency regulation and voltage regulation system controllers are also sent to this control block. Alternatively the droop line settings could have been adjusted for each VSC by the central controller directly. The PLL output angle (Theta) and the reference terminal voltage magnitude (Vtref) are used to calculate the injected current from the power. In the system simulated, two limit blocks are used to limit the power injection (active power limits ±10 kW, reactive power limits ±20 kVA). These limits are important during transient period of a disturbance in the system (figure 15).

6. The need for energy storage

A Microgrid will encounter a number of problems during operation; due to normal load and supply changes, also when switching from grid-fed to islanding mode. To maintain the voltage and frequency within the limits of a normal grid system, it will be necessary to have some form of temporary, rapid-response power injection. This is analogous to spinning reserve in a conventional power system but, due to the relatively low ratio of kinetic energy to power fluctuations in the Microgrid, fast response of the VSC (voltage source controller) is necessary. Generation with a fast response, rapidly increasing or decreasing real power produced, could in theory be used for this. The difficulty would lie in obtaining adequate speed of response at an acceptable price. The generator owner would also wish to maximize his payback, which would mean generating maximum real power whenever possible.

Consider an islanded microgrid in which (to maximize payback on investment) micro-sources are generating at their maximum real power rating with all this power

being absorbed by the local load. The loss of one micro-source would cause a shortage of real power, which eventually will be remedied by load shedding; in the interim, the power shortfall must be derived from somewhere, and here energy storage is unavoidable. The combination of the VSC and energy storage can also control the frequency and phase angle of the Microgrid during the resynchronization with the main network (see § 7). As well as being able to absorb or inject real power, the unit can provide reactive power compensation. In an unbalanced Microgrid, the energy storage device (which would preferentially be connected close to the connection transformer and breaker, § 1, figure 1), could also perform unbalanced current compensation.

There are a number of types of energy storage devices, that could be used to provide transient support; these include ultra-capacitors and SMES, however, a very strong contender, based on costs, steady state losses, energy density, power density and cycling capability, is the high-speed flywheel. An example is the unit shown in figure 16.

The main component of the high-speed flywheel is a high mass composite cylinder that is wound using a combination of carbon and glass fibre. The carbon layer gives the rotor the required strength to rotate at high speeds with the glass layer providing the extra mass. The centre bore of the cylinder is loaded with neodymium iron boron (permanent magnet powder) that provides the magnetic medium for the motor generator. A corresponding three-phase stator completes the motor generator design. The rotating cylinder operates within a high vacuum to minimize drag losses. The rotor is able to operate at a maximum speed of 37 800 rpm, store up to 14 MJ of energy and transfer power at up to 200 kW. The dc link voltage between the VSC and the KESS is used to control the power flow as shown in figure 17. The KESS monitors the dc link voltage and adjusts the power based on the profile (figure 17).

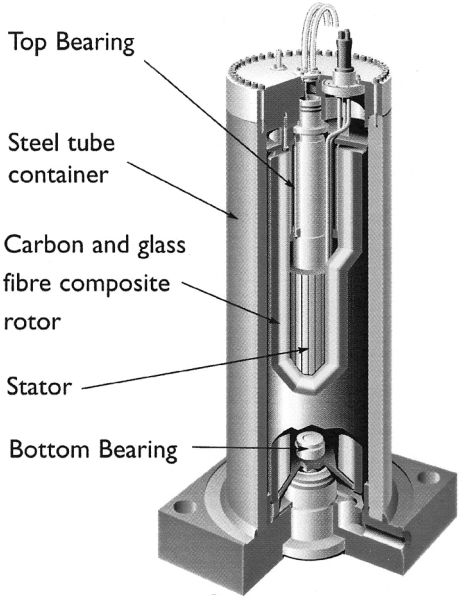

Figure 16. UPT KESS, (kinetic energy storage system).

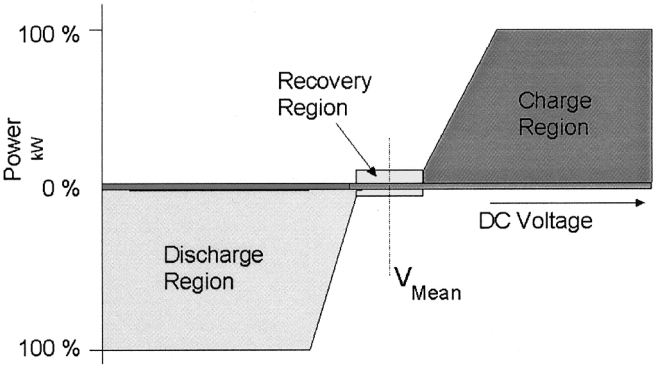

Figure 17. KESS power profile.

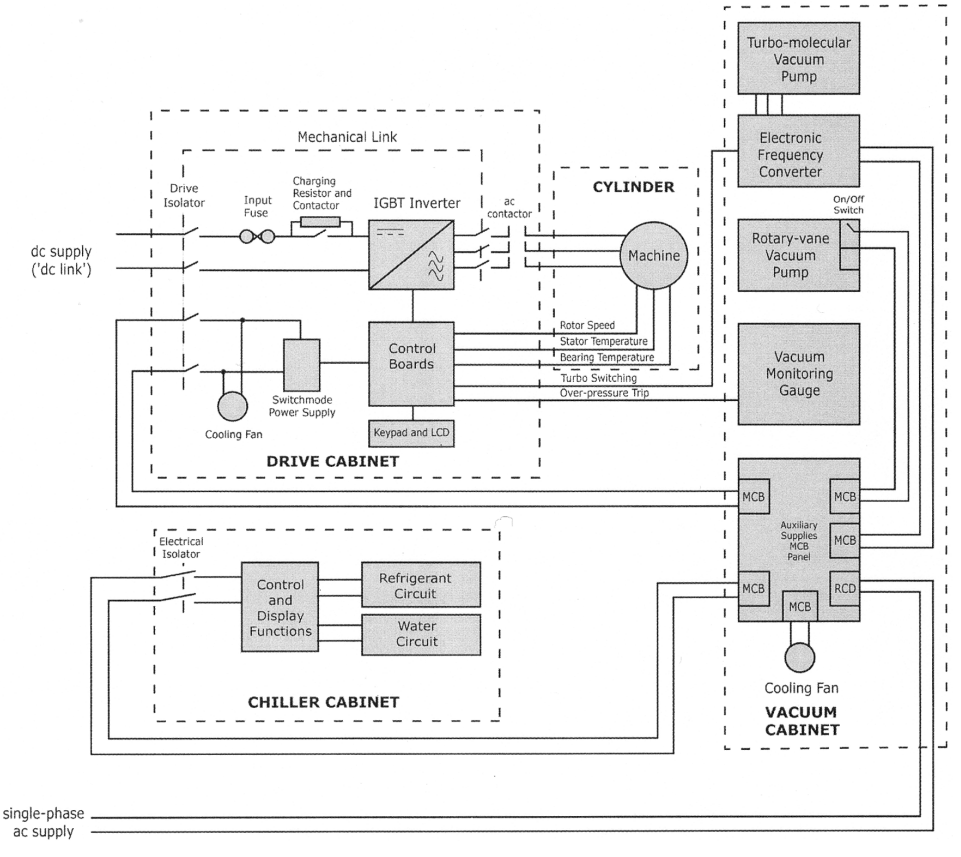

Figure 18. KESS schematic of the system.

Figure 18 shows the KESS system. The electric machine is shown as the 'cylinder' block. This is fed by a fast response power electronic inverter drive. A vacuum cabinet is required to evacuate the cylinder and reduce drag losses. An auxiliary chiller is also required for this.

The control electronics shown in figure 18, consist of a conventional three-phase IGBT voltage source inverter which interfaces the ac motor/generator to the dc link.

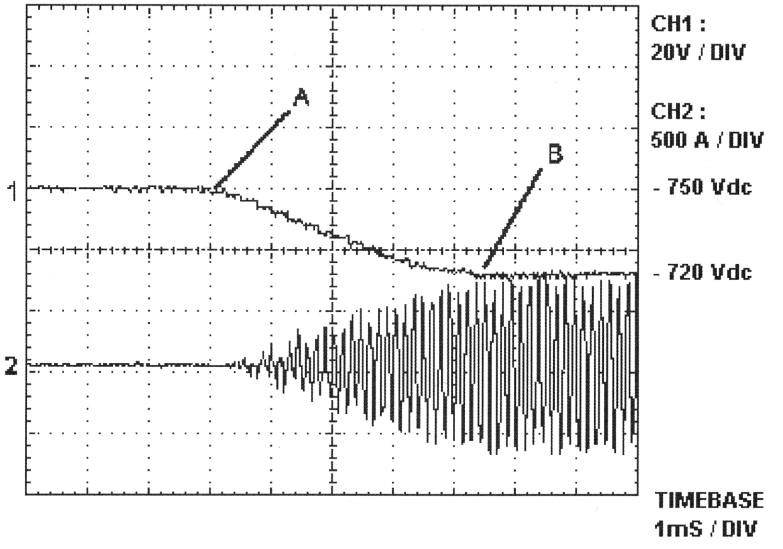

Figure 19. KESS (kinetic energy storage system) response to a dip in the dc link. Channel 1: dc link voltage, Channel 2: ac motor current on KESS, timebase: 1 ms/division, (A: loss of 'dc link' supply, B: KESS at full power).

Asynchronous PWM is employed at a fixed frequency of 8 kHz to drive the cylinder up to the lower operating frequency of around 30 000 rpm. At higher frequencies, synchronous PWM is employed at the electrical frequency, i.e. six times the mechanical speed or 3 to 3.78 kHz. This type of switching minimizes the losses produced when changing between mechanical and electrical energy.

Rapid response of the KESS is essential, since it will be mainly used to smooth out rapid transients, which occur in a grid system. Figure 19 shows how the KESS responds to a rapid fall in the dc link. Here a load of 200 kW was placed on the dc link, which, in turn was fed from a controlled rectifier. At point 'A' the rectifier was disconnected, the voltage then falls at a rate determined by the capacitance of the dc link. The KESS immediately detects the loss of the supply and starts to feed current into the link; in 4.5 ms the KESS is at full power supporting the dc link at the control voltage. In the microgrid installation, the KESS VSC will be controlling the dc link; this experiment shows that the KESS unit is clearly able to respond quickly enough to fulfil the rapid response requirements of the Microgrid. It will allow the power flow to be regulated by a fast acting real power vs. frequency characteristic.

7. Semi-autonomous microgrid operation

Should the main network experience an outage, or power quality problems, the Microgrid could disconnect, operating in autonomous mode. When the main network recovers, the Microgrid can then reconnect provided the Microgrid and network voltages are synchronized.

7.1. *On-set of autonomous microgrid operation due to a fault on the main network*

Figure 20 shows measured system frequency, rms terminal voltage, active and reactive power of the VSC, generator and load during islanded operation of the

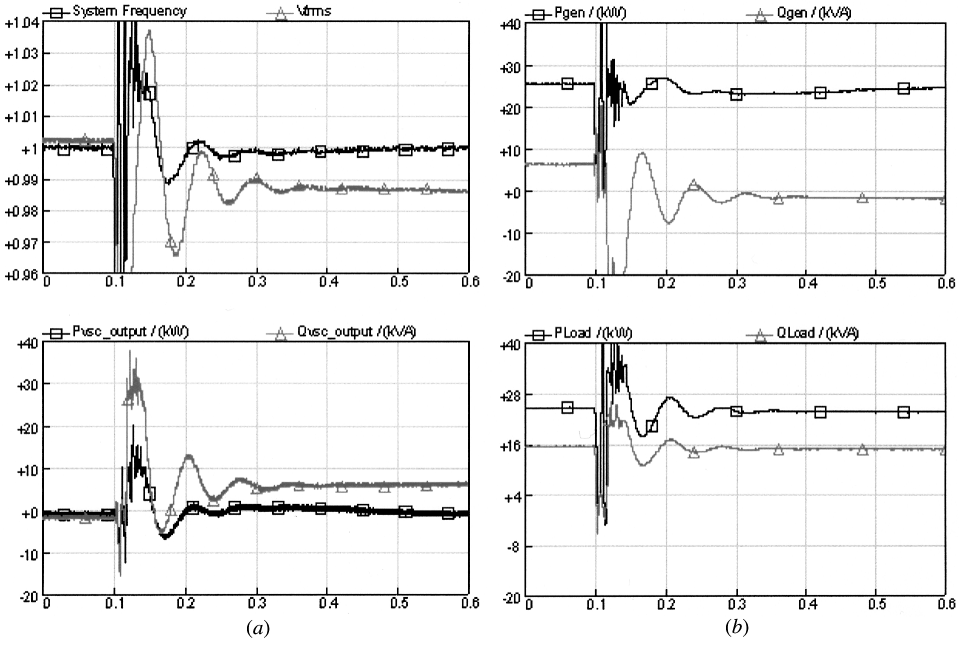

Figure 20. Simulation results when the micro grid is first disconnected from the main supply network (onset of autonomous operation), (*a*) system frequency, terminal voltage, injected VSC active and reactive power, (*b*) Active and reactive power supplied by the generator and absorbed by the Load.

Microgrid. Figure 21 shows three-phase instantaneous terminal voltage and current in the VSC circuit, generator, load and main supply. It has to be noted that the Microgrid absorbs significant amounts of current (20 A) from the main supply. Due to this, disconnection of the main supply impacts on the microgrid and a transient period can be observed from these figures. The frequency measurement from the PLL (based on voltage vector information) will not be very accurate during the transient period.

Powers in figure 20 are calculated from instantaneous phase variables, followed by a filtering stage. Frequency is derived from the phase angle of a phase-vector technique phase-locked loop (Manitoba Research Centre 2003). Since the phase variables deviate considerably from the sinusoidal during the first two cycles after disconnection, the frequency and power graphs during this stage contain a considerable amount of noise. Thereafter the signals settle to a second-order transient response to the change, determined by the interaction of the synchronous generator and the low-pass the filtering applied to the power signals.

7.2. *Resynchronization of microgrid*

Let us assume, that under islanded operation the energy storage device VSC injects zero active power, so that the embedded generators supply the total power required by the microgrid loads. During resynchronization, the energy storage unit VSC control slowly shifts the microgrid system frequency reference value (Fsystemref) to the main network frequency value and varies the VSC

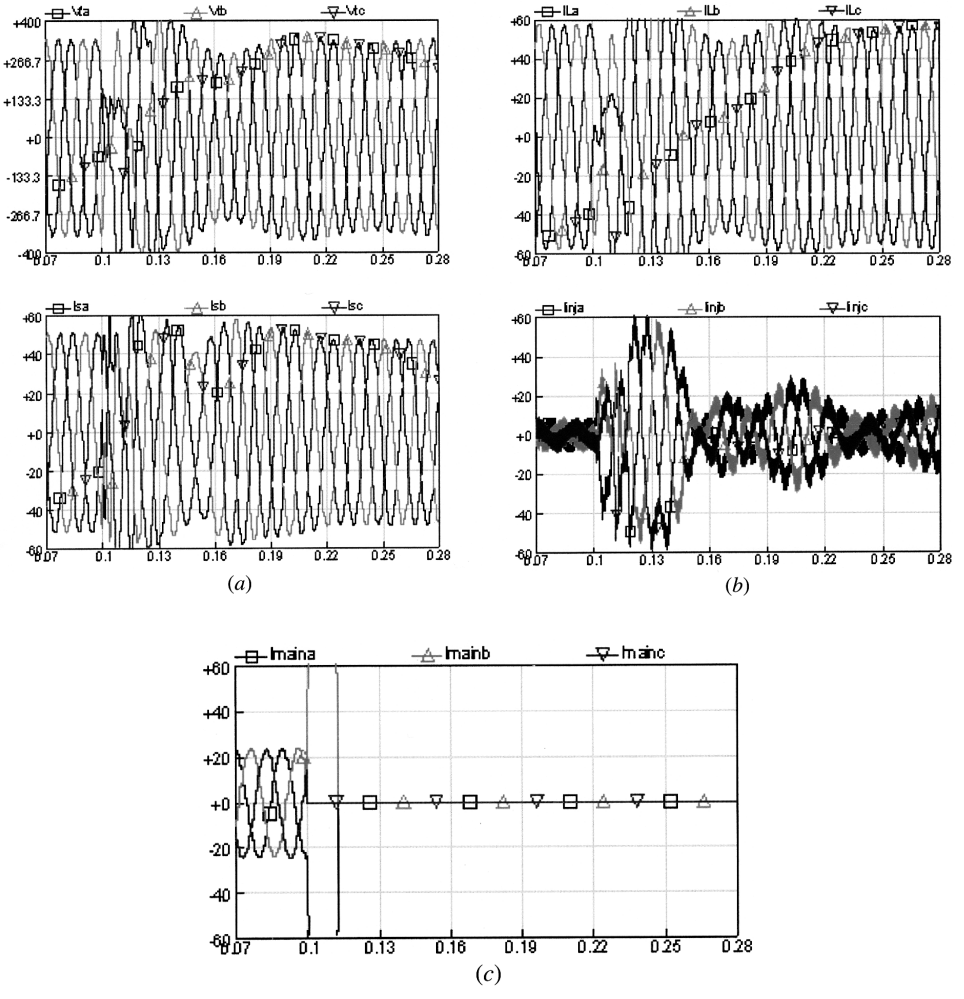

Figure 21. Simulation results when the Microgrid was disconnected from the main supply network (islanding operation), (*a*) terminal voltage, supply current from the Microgrid, (*b*) load current and VSC output current, (*c*) main supply network current.

injected active power accordingly. To satisfy the total active power requirement of the Microgrid, the active power supply from the embedded generators varies according to their power vs. frequency droop lines (§ 3). This introduces a slight variation on the microgrid system frequency (Fsystem) to synchronize the phase angle of the microgrid supply voltages (Vmga, Vmgb, Vmgc) to the main supply voltages (Vmaina, Vmainb, Vmainc), which are measured on both sides of the circuit breaker. When both frequencies and phase angles are locked, the breaker can be closed.

Figure 22 shows the block diagram of the synchronizing control. Three-phase instantaneous voltages on both sides of the circuit breakers are measured and fed as inputs to the controller. The PLL output angle (θ) is used to calculate the q-axis voltage components of both measured three-phase voltages. The difference between the q-axis voltages, is used as the error signal to synchronize both the

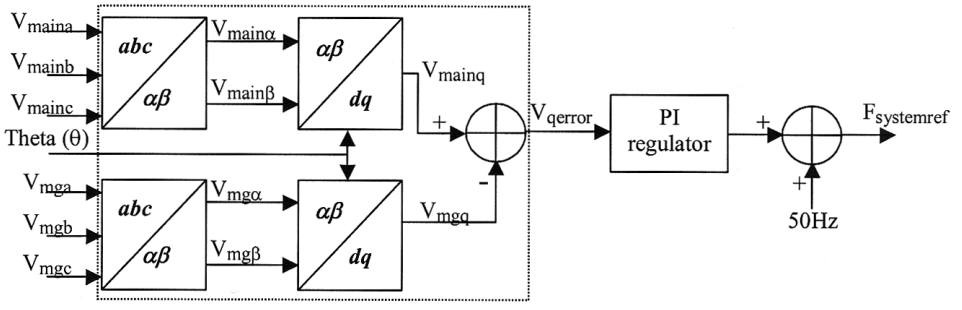

Figure 22. Block diagram of the VSC synchronizing control to reconnect the micro grid to the main supply.

main and Microgrid supply voltages. A PI regulator is used to regulate the error signal to zero by shifting the reference system frequency (Fsystemref). When the error signal is within the acceptable limits, the circuit breaker is closed. In the simulation used, the circuit breaker was switched on if the following conditions were satisfied

1. Magnitude of the main supply voltage (Vmainmag) should be above 90% of its rated value.

$$V_{\text{mainmag}} = \sqrt{V_{\text{main}\alpha}^2 + V_{\text{main}\beta}^2} \times \frac{100}{0.415} > 90$$

2. Error q-axis voltage component should be less than 5% (to ensure an appropriate synchronizing condition)

$$V_{\text{qerror}} = \left(V_{\text{mainq}} - V_{\text{mgq}}\right) \times \frac{100}{0.415} < 5$$

where

$$V_{\text{mainq}} = V_{\text{main}\beta} \times \cos\theta - V_{\text{main}\alpha} \times \sin\theta$$
$$V_{\text{mgq}} = V_{\text{mg}\beta} \times \cos\theta - V_{\text{mg}\alpha} \times \sin\theta$$

3. A period of at least 0.2 s has passed since the voltage on the main network supply has been restored. This period starts as soon as $V_{\text{mainmag}} > 90\%$. It is used to prevent a malfunction of the circuit breaker operation during any transient period.

Clearly the above scheme involves a degree of approximation, but, as perfect synchronization is not usually required, this is acceptable.

Figure 23 shows measured system frequency, rms terminal voltage (Vtrms), active and reactive power of the VSC, generator and load during sychronizing and reconnection operation of the Microgrid. It is assumed that disconnection occurs due to a fault on the main network which is subsequently removed. The real power control of the Microgrid was engaged as soon as the main network recovered from the fault. After a delay of at least 0.2 s the Microgrid is allowed to reconnect if its phase shift is within an acceptable deviation from that of the main

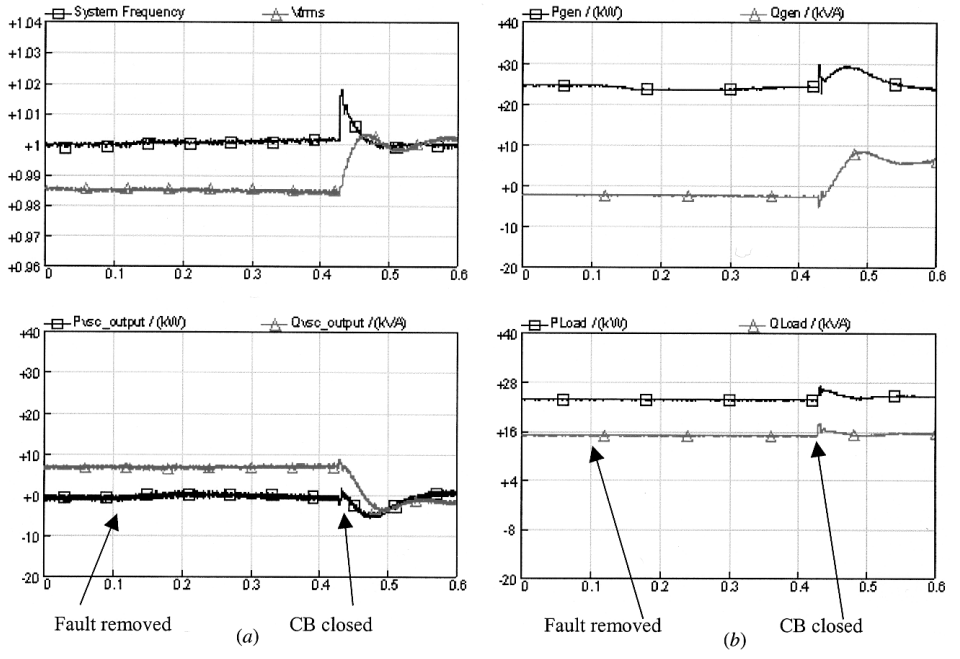

Figure 23. Simulation results when the micro grid was synchronized and reconnected to the main supply network (reconnecting operation, power and frequency), (*a*) system frequency, terminal voltage, injected VSC active and reactive power, (*b*) Active and reactive power supplied by the generator and absorbed by the Load.

network. When the reconnection occurs, the weaker network (the Microgrid) experiences a phase jump as a result, seen here as a frequency jump (figure 23).

Figure 24 shows three-phase instantaneous terminal voltage and current in the VSC circuit, generator and load. These figures show a smooth transfer at 0.43 s.

Figure 25 shows control parameter variation and main supply current during the resynchronizing of the Microgrid. A delay is introduced by the counter, which increases linearly, to a threshold value 100. The circuit breaker signal (CBsignal) goes high after satisfying both a counter delay (>100) and a reduced q-axis voltage magnitude (<5) requirement. This confirms that the Microgrid is reconnected when both Microgrid and main supply voltages are close to the synchronized condition. After reconnection, the main network sets the frequency and real power injection/absorption by the energy storage devices is not required, indeed the energy storage devices can use this period to 'recharge'.

8. Conclusions

Means to implement various functions of the Microgrid concept have been discussed including real power flow control, reactive power flow control, autonomous operation and resynchronization to the main network. This has been demonstrated using simulation and some experimental results. In a practical Microgrid some form of low bandwidth central controller is required to effect some of these functions, as is energy storage with an associated VSC.

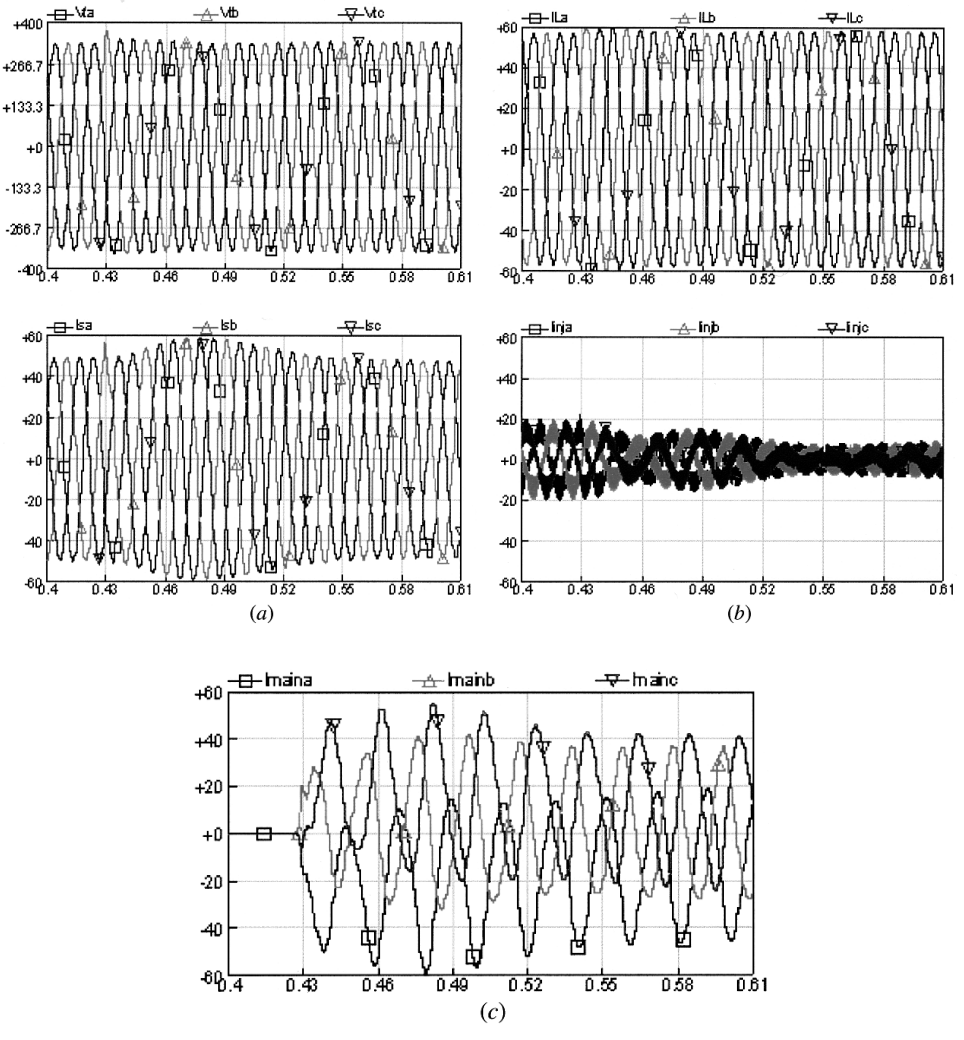

Figure 24. Simulation results when the micro grid was synchronized and reconnected to the main supply network (reconnecting operation, voltages and currents), (*a*) terminal voltage, supply current from the micro grid, (*b*) load current and VSC output current, (*c*) main supply network current.

Significant problems remain such as an understanding of systems stability, protection, and unbalanced current compensation. Assumptions, such as the degree to which the system can be considered to have a high X/R ratio, with a largely inductive line, do not always match all practical cases closely.

Acknowledgements

The authors would like to acknowledge the support for this research received from the European Union as part of project NNE5-2001-00463 'Microgrids', contract ENK5-CT-2002-00610.

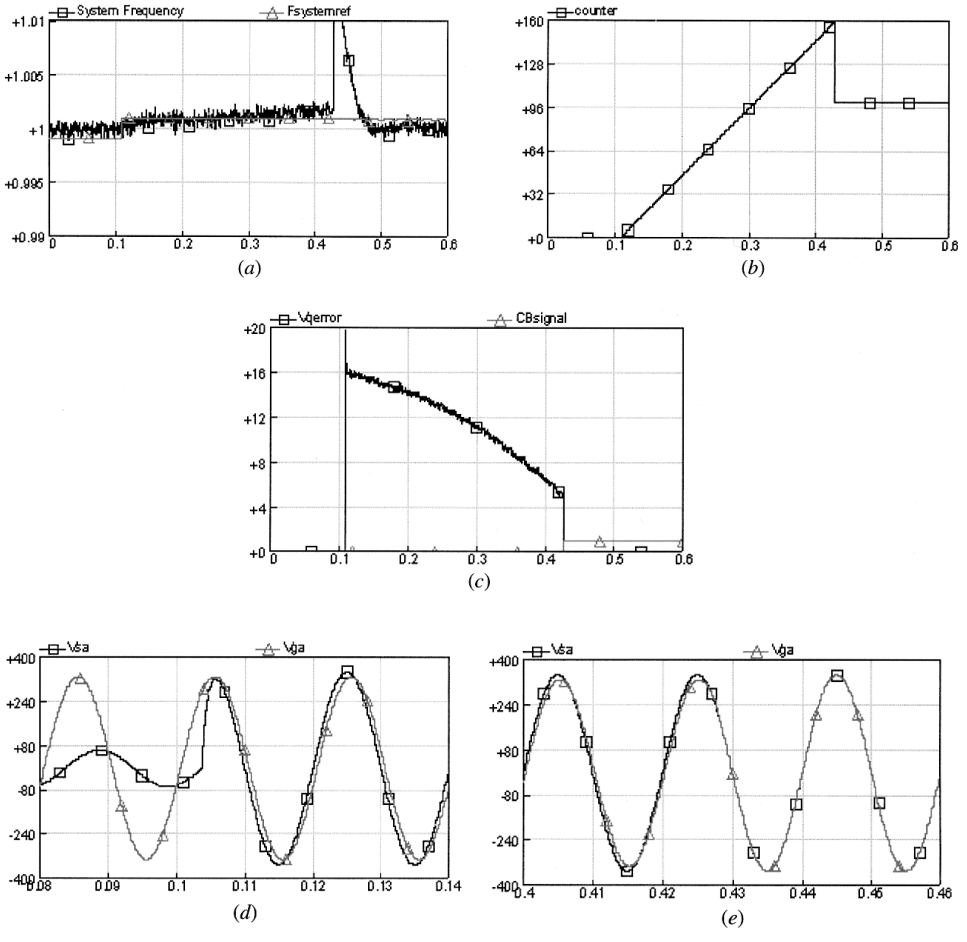

Figure 25. Simulation results when the micro grid was synchronized and reconnected to the main supply network (reconnecting operation, voltages and frequencies), (*a*) measured system frequency and reference frequency (no load system frequency), (*b*) counter to introduce delay during the transient period, (*c*) q-axis voltage component and circuit breaker signal, (*d*) main supply voltage and micro grid voltage when fault is removed, (*e*) main supply voltage and micro grid voltage when they were reconnected.

References

Chandorkar, M.C., Divan, M.D., and Adapa, R., 1993, Control of Parallel Connected Inverters in Standalone ac Supply Systems, *IEEE Transactions on Industry Applications*, **29,** 136–143.

Engler, A., Hardt, C., Strauß, P., and Vandenbergh, M., 2001, Parallel operation of generators for stand-alone single-phase hybrid system. *EPVSEC Conference*, Munich, Germany.

Engler, A., 2003, Vorrichtung zum gleichberechtigten Parallelbetrieb von ein- oder dreiphasigen Spannungsquellen, German Patent (pending) No.: 101 40 783.1

Johnson, B.K., Lasseter, R.H., Alvarado, F.L., Divan, D.M., Singh, H., Chandorkar, M.C., and Adapa, R., 1994, High-temperature Superconducting dc networks, *IEEE Transactions on Applied Superconductivity*, **4,** 115–120.

LASSETER, B., 2001, Microgrids distributed power generation. *IEEE Power Engineering Society Winter Meeting Conference Proceedings*, Columbus, OH, USA, **1,** 146–149.

LASSETER, R., AKHIL, A., MARNAY, C., STEPHENS, J., DAGLE, J., GUTTROMSON, R., Meliopoulos, A.S., Yinger, R., and Eto, J., 2002 a, White paper on integration of distributed energy resources—the CERTS MicroGrid concept, Office of Power Technologies of the US Department of Energy, Contract DE-AC03-76SF00098.

LASSETER, R.H., 2002 b, MicroGrids, IEEE Power Engineering Society Winter Meeting Conference Proceedings, New York, NY,USA **1,** 305–308.

MANITOBA, HVDC Research Centre Inc, 2003, Three-phase PI-controlled phase locked loop, PSCAD/EMTDC version 4.0.1 Manual.

TYLL, H., and Bergmann, K., 1990, Use of static VAR compensators (SVCs) in high voltage systems, SRBE-KBVE Studiedag, Brussels.